

# THE STATISTICAL ANALYSIS OF FLAPPING PHENOMENON IN A TWO-DIMENSIONAL TURBULENT JET

**Osamu Terashima**

Department of Mechanical Science and Engineering  
Nagoya University  
Furo-cho, Chikusa-ku, Nagoya-shi, Aichi, 464-8603, Japan  
o-terashima@mech.nagoya-u.ac.jp

**Yasuhiko Sakai and Kouji Nagata**

Department of Mechanical Science and Engineering  
Nagoya University  
Furo-cho, Chikusa-ku, Nagoya-shi, Aichi, 464-8603, Japan  
ysakai@mech.nagoya-u.ac.jp, nagata@nagoya-u.ac.jp

## ABSTRACT

The characteristics of a two-dimensional turbulent jet in flapping motion are investigated by simultaneous measurement of the velocity and the pressure. The simultaneous measurements are performed by using a combined probe, which was developed by our laboratory (Terashima et al., 2010), that consists of an X-type hot-wire probe and a static pressure probe. The measured data are analyzed by using conditional-sampling technique and ensemble-averaging technique, on the basis of an intermittency function to determine whether the jet is flapping or not. The intermittency function is obtained by applying a continuous wavelet transform with Gabor mother wavelet to the measured signals of hot-wire anemometers set in the self-preserving region of the jet.

The measured results obtained by the present new method show that the characteristics of the flapping motion clearly, and the ensemble-averaged velocity field during the flapping motion shows a good agreement with the results obtained by Sakai et al. (2006) through the multi-point simultaneous measurement of the velocity. Further, the ensemble-averaged static pressure field in the flapping motion indicates the existence of a coherent vortex structure, which is interpreted as a combination of flapping and puffing motion in the self-preserving region. The statistical analysis of the flapping motion shows that the flapping motion arises at random, and the average interval time of the arising of the flapping motion is about 6.1 times the flapping periods (0.24 sec), and the average duration time of the flapping motion is about 1.7 times the flapping period (0.07 sec) and the one that continues over 3.0 times the flapping period is very few. Moreover, the two-points spatial velocity correlation, which becomes negative value, substantially depends on whether the flapping motion arises or not. These results indicate that the flapping motion in a two-dimensional turbulent jet has a very important role to the properties of the jet, although the flapping motion is a rare phenomenon.

## INTRODUCTION

The flapping motion is one of the coherent structure in the self-preserving region of a two-dimensional turbulent jet (Goldschmidt et al., 1973; Antonia et al., 1983; Oler et al., 1982). The term “flapping” was named from the visual image of this phenomenon that the jet flaps as a flag does. There were almost no researches by which the entity of the flapping motion could be captured until the multi-point simultaneous measurement of the velocity in the two-dimensional turbulent jet by Sakai et al. (2006). The measured velocity field by Sakai et al. showed that there existed a pair of fluid lumps with the positive and negative streamwise velocity fluctuation on the opposite sides of the jet centerline, and the signs of the fluid lumps changed alternately as time proceeds. Furthermore, on the basis of the result of the Karhunen-Loève (KL) expansion, a new interpretation of the coherent structure model in the self-preserving region of a two-dimensional turbulent jet which was given from the combination of “flapping motion” and “puffing motion” (Sakai et al., 2006). However, the cause of occurrence and the characteristics of the flapping motion were still not clear.

From this point of view, in this study, the detail characteristics of the flapping motion are investigated to clarify the cause of the arising of the flapping motion. Firstly, the new method to discriminate the flapping motion and determine the intermittency function about the arising of the flapping motion by using the continuous wavelet transform with Gabor mother wavelet is developed. Secondly, the ensemble-averaged velocity and the pressure field on the basis of the intermittency function obtained by the present new method are investigated, and the validity of the present method is confirmed. Thirdly, the interval time and the duration time of the arising of the flapping motion are estimated. Finally, to clarify the trigger of the arising of the flapping motion, the pressure fluctuation near the nozzle exit just before the flapping motion starts or ends, and the relationship between the pressure fluctuation

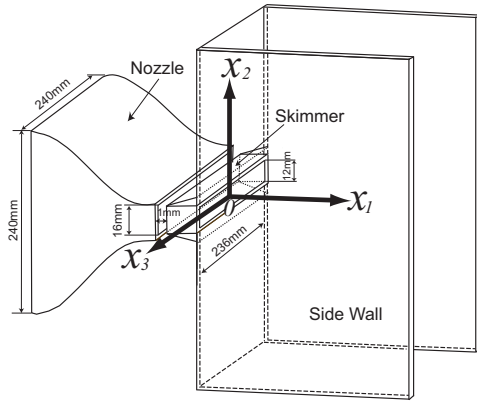


Figure 1. Schematic view of the apparatus and coordinate system of the two-dimensional jet.

and the arising of the flapping motion are examined. The understanding of the details of the flapping motion by this study has the possibility to contribute the effective control of the jet to enhance the turbulent mixing of the jet.

## EXPERIMENTAL SETUP AND PROCEDURE

### Two-dimensional turbulent jet

Figure 1 shows the schematic view of the experimental apparatus and the coordinate system of the two-dimensional jet. The height  $d$  and the width  $l$  of the exit of the skimmer, which was set to eliminate the boundary layer develops along the contraction nozzle, were 12 mm and 236 mm, respectively. The velocity  $U_0$  at the skimmer exit was about 27.5 m/s and the Reynolds number  $Re$  (defined as  $U_0 d/\nu$ ;  $\nu$  was kinematic viscosity) was about 22,000. By use of the skimmer and the side wall, a uniform velocity profile at the skimmer exit and a good two dimensional flow field in the test section could be realized. The coordinate system was as follows: the axial (streamwise) coordinate was  $x_1$ , the vertical (cross-streamwise) coordinate was  $x_2$ , and the spanwise coordinate was  $x_3$ .

In this study, two I-type hot-wire probes (hereafter called “detectors”) were set at the intermittent region ( $x_1/d=40$ ) to detect the flapping motion as shown in Fig. 2. In addition, the combined probe (will be shown next section in detail) for the simultaneous measurement of the velocity and the pressure which was connected to the traverse system was set in the measurement region. By use of the stepping motor to move the traverse system, the high accurate spatial measurement was realized. The sampling frequency of the velocity and the pressure by the combined probe and the velocity by the detector were 20 kHz and the number of sampling data was 262,144. The measured data were saved on the hard disk of a personal computer via an A/D converter, and then the data were analyzed.

### Combined probe

Figure 3 shows the combined probe for the simultaneous measurement of the velocity and the pressure. The static pressure probe was placed between two hot-wires (diameter:

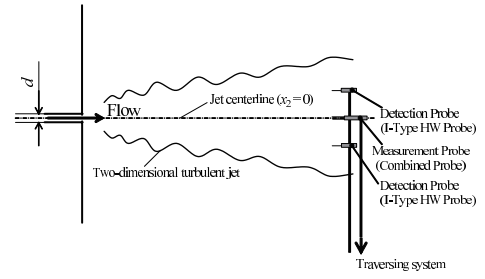


Figure 2. Schematic view of the measurement apparatus.

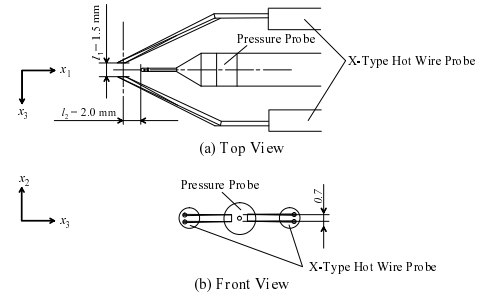


Figure 3. Schematic view of the combined probe. (a) Top view and (b) front view.

$5.0\mu\text{m}$ , length: 1.0 mm) which constructed the X-type hot-wire sensor to measure two velocity components. The gap between the side wall of the static pressure tube and the hot-wire  $l_1$  was 0.50 mm, and the streamwise gap between the tip of the static pressure tube and the cross point of the two hot-wires  $l_2$  was 2.0 mm. These gaps are necessary to eliminate the interference between each probe because the disturbances caused by one probe influenced the measurement accuracy of another probe in some cases (Terashima et al., 2010). Note that in this case, there is a time lag between the signals of velocity fluctuation and the pressure fluctuation. Therefore, the time lag was corrected by using the Taylor’s hypothesis. Further, it should be noted that from the previous experimental results of this two-dimensional jet (Sakai et al., 2007), the Taylor transverse microscale and Kolmogorov microscale were estimated to be approximately 3.0 mm and 0.10 mm respectively, in the self preserving region. Therefore, judging from the diameters and the arrangement of the probe, it is considered that the spatial resolution of the velocity and the pressure fluctuation by this probe is as large as the Taylor microscale.

Figure 4 shows the schematic view of the pressure probe which used in the combined probe shown in Fig.3. The shape of the tip of the pressure tube was hemispherical like that of the pitot tube. The external and internal diameter of the pressure tube was 0.50 mm and 0.34 mm, respectively. There were eight static holes on the sidewall of the pressure tube and the diameter of each static hole was 0.20 mm. Four of these holes were located at 0.75 mm from the tip, and the others were at 1.25 mm from the tip and they were inclined at 45 degrees to the first four holes as shown in Fig. 4. A microphone of the diameter was 2.54 mm, which acted as a pressure sensor, was

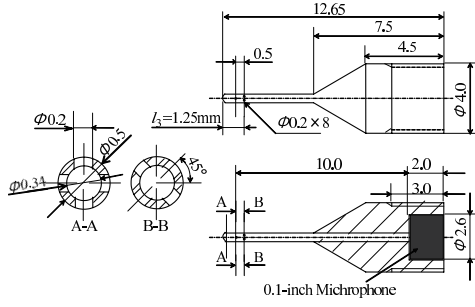


Figure 4. Schematic view of the pressure probe.

embedded inside the flare of the static pressure probe. The sensitivity of the microphone was 16.0 mV / Pa. Here, we should note that the modulation of the amplitude and the phase shift of the pressure fluctuation signal, which were caused by the Helmholtz (3,500 Hz) and Organ pipe resonances (17,000 Hz), occurred in the pressure tube. Therefore, those modulations were digitally corrected by using Fourier series (Sakai et al., 2010) in this study.

### Frequency of the flapping motion

Several techniques to determine the frequency of the flapping motion ( $f_p$ ) in the self-preserving region of the two-dimensional turbulent jet have been suggested. In this study, the method which uses the peak frequency of the power spectrum of the cross-streamwise velocity fluctuation on the jet centerline to estimate  $f_p$  was adopted because the damping characteristic of the flapping frequency toward streamwise direction was evaluated more accurately than other methods. Here, the damping characteristic of the flapping frequency toward the streamwise direction means that the flapping frequency is proportional to the  $-3/2$  power law for the dimensionless value of the streamwise location ( $x_1/d$ , defined as  $X$ ). This characteristic can be derived by some characteristics of the jet in followings; (1) downstream variation of the half width of the cross-streamwise profile of the mean streamwise velocity  $b$ , i.e.,  $b$  is proportional to  $X$  ( $b \propto X$ ); (2) downstream variation of the streamwise velocity on the jet centerline, i.e.,  $U_c$  is proportional to  $X^{-0.5}$  ( $U_c \propto X^{-0.5}$ ); (3) Strouhal number  $S_t$ , which defined as  $f_p b / U_c$ , in the self-preserving region is constant ( $S_t = \text{Const.}$ ). By the preliminary measurement of the cross-streamwise velocity fluctuation on the jet centerline, it was shown that the flapping frequency  $f_p$  was 25 Hz at the self-preserving region in the present jet ( $x_1/d=40$ ).

### Extraction of flapping motion

In the previous study (Sakai et al., 2006), the existence of flapping motion was confirmed by the multi-point simultaneous measurement of velocity. However, in the previous study, the flapping motion was captured by visually. Therefore, it was difficult to analyze the phenomenon statistically because visual capturing of the phenomenon was involved in the subjective view by the observer. From this point of view, the new method to extract the flapping motion by using the continuous wavelet transform with Gabor mother wavelet is developed to

eliminate the subjective view of the observer in the determination of the time which the flapping motion is arising. The procedure by present new method is shown in follows and Fig. 5 (a)-(d). Firstly, in the preliminary experiments, the frequency of the flapping motion  $f_p$  at the measurement point ( $x_1/d=40$ ) was estimated as the peak frequency of the power spectrum of the cross-streamwise velocity fluctuation on the jet centerline. Secondly, by applying the continuous wavelet transform with Gabor mother wavelet (see Eqs. 1 and 2) to the signals of streamwise velocity fluctuations measured by two I-type hot-wire probes ( $u_1(t)$  and  $u_2(t)$  in Fig. 5 (a)), the real parts of the wavelet component which corresponds to the flapping frequency  $f_p$  (defined as  $w_1(t)$  and  $w_2(t)$  in Fig. 5 (b)) are extracted. Thirdly, the product of  $w_1(t)$  and  $w_2(t)$  which is defined as the detection function  $D(t)$  (shown in Fig. 5 (c)) is calculated, then the intermittency function  $I(t)$  is decided by the suitable negative threshold. Finally, from the signs of  $w_1(t)$  and  $w_2(t)$  and the periodicity of  $I(t)$ , the flapping intermittency function  $I_f(t)$  is obtained. Here, the "negative threshold" is chosen so as for the ratio of the turbulent intensity in the duration time of the flapping motion to that in the total measurement time to become 23 %. This ratio was equal to the energy contribution ratio of the first mode of the KL expansion investigated by Sakai et al. (2006). In this study, the continuous wavelet transform with Gabor mother wavelet as follows is used,

$$W(a, b) = \frac{1}{\sqrt{a}} \int \phi\left(\frac{t-b}{a}\right) s(t) dt \quad (1)$$

$$\phi(t) = \frac{1}{2\sqrt{\pi}\sigma} \exp\left(-\frac{t^2}{\sigma^2}\right) \exp(-it) \quad (2)$$

where,  $a$ : scale parameter,  $b$ : time parameter,  $s(t)$ : time series signal,  $i$ : imaginary unit,  $\phi(t)$ : Gabor function,  $\sigma$ : parameter to decide the frequency resolution and the time resolution. In this study,  $\sigma$  was set equal to 6.

## RESULTS AND DISCUSSION

### Velocity field in the jet

Figure 6 shows the cross-streamwise profiles of the streamwise velocity  $U$ . The ordinate indicates  $U/U_c$ , and the abscissa indicates  $x_2/b$ . Hereafter the subscript "c" means the value on the jet centerline ( $x_2=0$ ), and  $b$  is the half-width of the cross-streamwise profile of the mean streamwise velocity. The solid line denotes a Gaussian profile. The measurements were performed at  $x_1/d=20, 30$ , and 40. From Fig. 6, it is found that the measured results show a good similarity and those are in good agreement with the Gaussian profile. Therefore, the validity of the measurement apparatus and measurement equipment is confirmed.

### Velocity and pressure field in flapping motion

Figure 7 shows the contour map of the conditional ensemble-averaged streamwise mean velocity  $U_{ens}$  measured

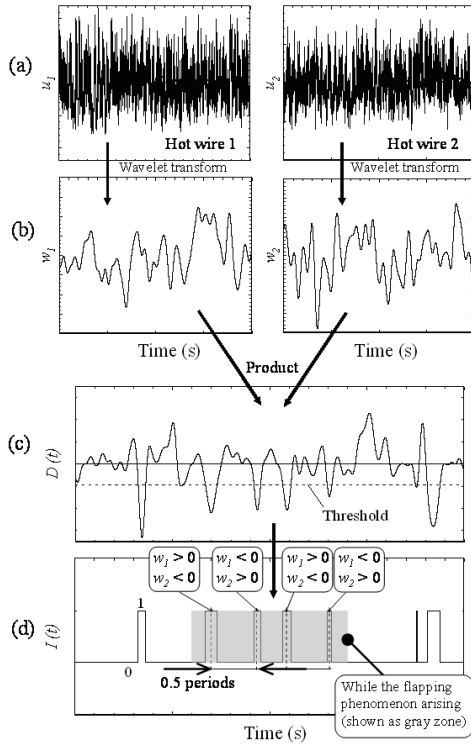


Figure 5. Signal processing for the decision of the intermittency function  $I(t)$ .

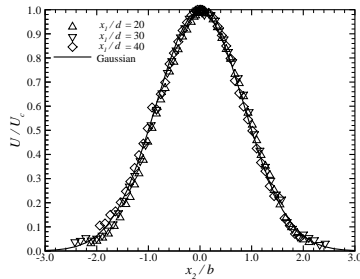


Figure 6. Cross-streamwise profiles of mean streamwise velocity  $U$  at  $x_1/d=20, 30,$  and  $40$ .

at  $x_1/d=40$ . The depth of shading in Fig. 7 exhibits the magnitude of  $U_{ens}$  normalized by  $U_c$ . The abscissa indicates the time from the flapping motion starts (i.e.,  $t=0$  means the time when the flapping motion starts) normalized by the flapping period  $T_p(=1/f_p)$  and the ordinate indicates  $x_2$  normalized by  $b$ . Hereafter the subscript “ens” indicates the conditional ensemble-averaged value.

Figure 8 shows the contour map of the conditional ensemble-averaged streamwise velocity fluctuation  $u_{ens}$  measured at  $x_1/d=40$ . The depth of shading in Fig. 8 exhibits the value of  $u_{ens}$  normalized by the RMS value of the streamwise velocity fluctuation on the jet centerline  $u'_c$ . The abscissa and ordinate are the same as those in Fig. 7.

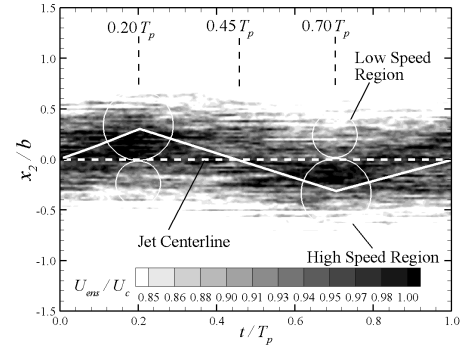


Figure 7. Ensemble-averaged streamwise velocity  $U_{ens}$ .

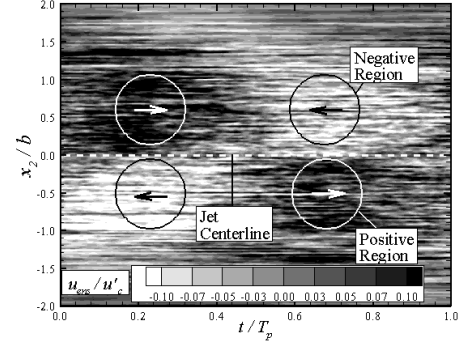


Figure 8. Ensemble-averaged streamwise velocity fluctuation  $u_{ens}$ .

Figure 9 shows the contour map of the conditional ensemble-averaged pressure fluctuation  $p_{ens}$  measured at  $x_1/d=40$ . The depth of shading in Fig. 9 shows the value of  $p_{ens}$  normalized by the RMS value of the pressure fluctuation on the jet centerline  $p'_c$ . The abscissa and ordinate are the same as those in Fig. 7.

From the results given above (Figs. 7 to 9), the following characteristics of the flapping motion are verified; (1) a pair of fluid lumps with the positive and negative streamwise velocity fluctuation exists on the opposite sides of the jet centerline; (2) the signs of the velocity fluctuation of those fluid lumps change alternately as the time advances. Therefore, it is confirmed that the present method is available to extract the flapping motion by use of the wavelet transform and the suitable negative threshold for the detection function.

### Interval and duration of flapping motion

Figure 10 shows the interval time between the arising of one flapping motion and next arising of the flapping motion. The abscissa indicates the interval time of the flapping motion normalized by the flapping frequency  $f_p$ , and the ordinate indicates the relative number of each interval time in the whole measurement time (26.2 seconds). Figure 10 indicates that the average interval time of the flapping motion was about 6.1 times the flapping period (0.24 seconds), and it is found that the flapping motion arises at random.

Figure 11 shows the duration time of one flapping motion. The abscissa indicates the duration time normalized by

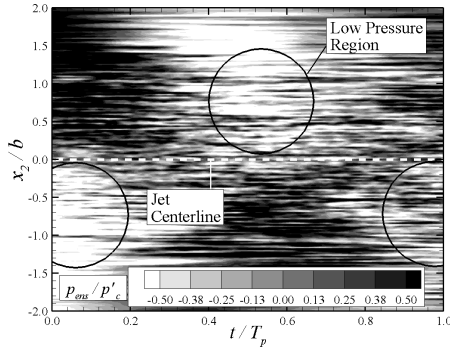


Figure 9. Ensemble-averaged pressure fluctuation  $p_{ens}$ .

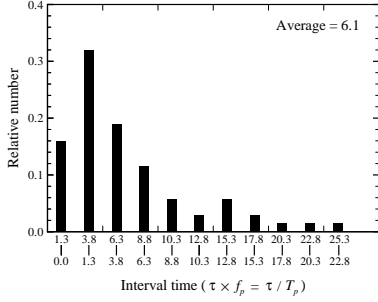


Figure 10. Interval time of the flapping motion.

the flapping frequency  $f_p$  and the ordinate indicates the relative number of each duration time in the whole measurement time. Figure 11 indicates that the most part of the flapping motion continued only 1.0 or 1.5 times the flapping period ( $T_p$ ) and the one that continues over 3.0 times the flapping period is very few. Further, the average duration time of the flapping motion was about 1.7 times the flapping period ( $1.7T_p$ ; about 0.07 seconds).

Next, we investigated the two-points velocity correlation by use of the two I-type hot-wire probes set as shown in Fig. 2. It was found that the value of two-points correlation was equal to -0.15. Note that this negative sign of the correlation is one of the characteristics of the two-dimensional jet observed by previous studies. On the other hand, it was equal to -0.33 during the time which flapping motion was arising and -0.09 during the time which flapping motion was not arising. These results indicate that the flapping motion plays an important role to the properties of the two-dimensional jet although it is rare phenomenon.

### Velocity and pressure fluctuation near the nozzle exit

Figure 12 shows the cross-streamwise profiles of the RMS value of the conditional ensemble-averaged streamwise velocity fluctuation  $u'_{ens}$ . The ordinate indicates  $u'_{ens}$  normalized by that on the jet center line  $u'_c$ . The abscissa indicates  $x_2/d$ . In Fig. 6, it is found that the averaged velocity and pressure field are symmetrical to the jet centerline. Therefore, only the profiles in the range of  $0 \leq x_2/d$  will be shown here. The measurements were performed at the position near the

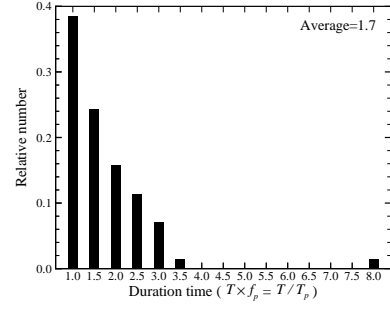


Figure 11. Duration time of the flapping motion.

nozzle exit ( $x_1/d = 0.1$ ). In Fig. 12, the solid line indicates the non-dimensional RMS value of the streamwise velocity fluctuation  $u'$ , the dashed line indicates  $u'_{ens}$  when  $I_f(t) = 1$  and the dash-dot line indicates  $u'_{ens}$  when  $I_f(t) = 0$ . Figure 12 indicates that the cross-streamwise profile of the RMS value of the streamwise velocity fluctuation depends on  $I_f(t)$ . It becomes large when  $I_f(t) = 1$  and it becomes slightly small when  $I_f(t) = 0$ .

Figure 13 shows the cross-streamwise profiles of the RMS value of the conditional ensemble-averaged pressure fluctuation  $p'_{ens}$ . The ordinate indicates  $p'_{ens}$  normalized by that on the jet center line  $p'_c$ . The abscissa indicates  $x_2/d$ . The measurements were performed at the position near the nozzle exit ( $x_1/d = 0.1$ ). In Fig. 13, the solid line indicates the non-dimensional RMS value of pressure fluctuation  $p'$ , the dashed line indicates  $p'_{ens}$  when  $I_f(t) = 1$  and the dash-dot line indicates  $p'_{ens}$  when  $I_f(t) = 0$ . Figure 13 indicates that the cross-streamwise profiles of the RMS value of the pressure fluctuation are almost same regardless of  $I_f(t) = 0$  or 1. This indicates that the RMS value of the pressure fluctuation near the nozzle exit does not strongly depend on  $I_f(t)$ .

Figure 14 shows the contour maps of the conditional ensemble-averaged pressure fluctuation  $p_{ens}$ . The depth of shading in Fig. 14 exhibits  $p_{ens}$  normalized by  $p'_c$ . The abscissa indicates the non-dimensional time  $t/T_p$ . Here,  $t$  in Fig. 14 (a) means the differential time from the time when flapping motion starts (i.e.,  $t = 0$  means  $I_f(t)$  becomes from 0 to 1) and  $t$  in Fig. 14 (b) means the differential time from the time when flapping motion ends (i.e.,  $t = 0$  means  $I_f(t)$  becomes from 1 to 0). The ordinate indicates  $x_2/d$ . Figure 14 (a) indicates that the strong negative pressure fluctuation arises just before the flapping motion started ( $-0.6 \leq t/T_p \leq 0.0$ ) at near the edge of the nozzle exit ( $x_2/d = 0.5$ ). On the other hand, Fig. 14 (b) indicates that the negative strong pressure fluctuation arises just before the flapping motion ended ( $-0.6 \leq t/T_p \leq 0.0$ ) at slightly far from the edge of the nozzle exit ( $x_2/d = 0.8$ ). These results show that there is a possibility that the strong negative pressure fluctuation near the nozzle exit is some trigger to the arising of the flapping motion.

### CONCLUSIONS

- The new method to extract the flapping motion is developed by using continuous wavelet transform, and the validity of this new method is confirmed.
- The ensemble-averaged static pressure field during the

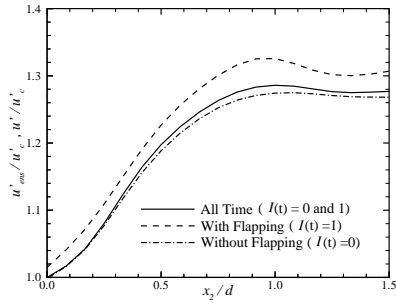


Figure 12. Cross-streamwise profiles of  $u'_{ens}/u'_c$  at  $x_1/d=0.1$ .

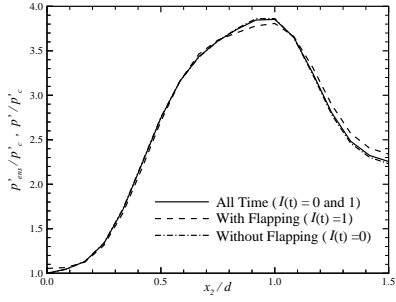


Figure 13. Cross-streamwise profiles of  $p'_{ens}/p'_c$  at  $x_1/d=0.1$ .

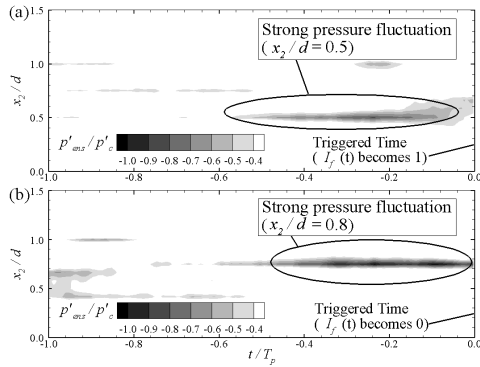


Figure 14. Contour maps of conditional ensemble-averaged pressure fluctuation  $p'_{ens}/p'_c$  at  $x_1/d=0.1$ . (a) Triggered time ( $t/T_p=0$ ) is when  $I_f(t)$  becomes from 0 to 1 and (b) triggered time is when  $I_f(t)$  becomes from 1 to 0.

flapping motion indicates the existence of a coherent vortex structure, interpreted as a combination of flapping and puffing motion in the self-preserving region of the jet.

- The flapping motion arises at random, and the average interval time of the arising of the flapping motion is about 6.1 times the flapping period  $T_p$  (0.24 sec).
- The average duration time of a flapping motion is about 1.7 times the flapping period  $T_p$  (0.07 sec) and the one that continues over 3.0 times the flapping period  $T_p$  is very few.
- The conditional ensemble-averaged pressure fluctuation

near the nozzle exit just before the flapping motion starts or ends indicates that there is a possibility that the arising of the flapping motion depends on the strong negative pressure fluctuation observed near the nozzle exit.

## ACKNOWLEDGMENTS

The authors express their gratitude for partial financial support of this study by the Ono Acoustic Research Fund, the Grant-in-Aids for scientific research (No.22360076, No.22360077 and No.23760155), Hitachi, Ltd., and also express their appreciation to Mr. Shouji Yuichi and Onishi Kazuhiro (Graduate school students in Nagoya University) who supported this experiment.

## REFERENCES

- Antonia, R.A., Browne, L.W.B., Rajagopalan, S., Chambers, A.J., 1983, "On the organized motion of a turbulent plane jet", *Journal of Fluid Mechanics*, Vol.134, pp.49-66.
- Goldshmidt, V.W., Bradshaw, P., 1973, "Flapping of a plane jet", *Physics of Fluids*, Vol.16, No.3, pp.354-355.
- Oler, J.W., Goldshmidt, V.W., 1982, "A vortex-street model of the flow in the similarity region of a two-dimensional free turbulent jet", *Journal of Fluid Mechanics*, Vol.123, pp.523-535.
- Sakai, Y., Tanaka, N., Kushida, T., 2006, "On the Development of Coherent Structure in a Plane Jet (Part2, Investigation of Spatio-Temporal Velocity Structure by the KL Expansion)", *JSME International Journal, Series B*, Vol.49, No.2, pp.714-721.
- Sakai, Y., Tanaka, N., Yamamoto, M., Kushida, T., 2006, "On the Development of Coherent Structure in a Plane Jet (Part3, Multi-point Simultaneous Measurement of Main Streamwise Velocity and Reconstruction of Velocity Field by the KL Expansion)", *JSME International Journal*, Vol.49, No.3, pp.722-730.
- Sakai, Y., Tanaka, N., Yamamoto, M., Kushida, T., 2006, "On the Development of Coherent Structure in a Plane Jet (Part4, The Multipoint Simultaneous Measurement of Two-Component Velocities and the Simple Coherent Structure Model)", *JSME International Journal*, Vol.49, No.4, pp.899-905.
- Sakai, Y., Moriguchi, Y., Tanaka, N., Yamamoto, M., Kubo, T., Nagata, K., 2007, "On Characteristics of Velocity and Pressure Field in Two-Dimensional Turbulent Jet", *Journal of Fluid Science and Technology*, Vol.2, No.3, pp.611-622.
- Sakai, Y., Nagata, K., Moriguchi, Y., Kubo, T., 2010, "Study on the structure of turbulent jet by the simultaneous measurement of instantaneous two velocity components and static pressure", *Proceedings of Int. Conf. on Jets, Wakes and Separated Flows, ICJWSF2010, Cincinnati, Ohio USA, CD-ROM*.
- Terashima, O., Sakai, Y., Shouji, Y., Kojima, Y., Nagata, K., and Kubo, T., 2010, "Development of the innovative probe for the simultaneous measurement of instantaneous pressure and two velocity components", *Proceedings of Int. Conf. on Jets, Wakes and Separated Flows, ICJWSF2010, Cincinnati, Ohio USA, CD-ROM*.